

WATER-SOLUBLE SAND CORE MADE BY BINDER JETTING PRINTING WITH THE BINDER OF POTASSIUM CARBONATE SOLUTION

Long Zhang

Anhui Province Key Laboratory of Metallurgical Engineering & Resources Recycling, Anhui University of Technology, Ma'anshan 243002, China

School of Metallurgical Engineering, Anhui University of Technology, Ma'anshan 243002, China

Xiaona Yang, Lina Zhang, Chunyang Hu and Hao Wang

School of Metallurgical Engineering, Anhui University of Technology, Ma'anshan 243002, China

Songlin Ran 

Anhui Province Key Laboratory of Metallurgical Engineering & Resources Recycling, Anhui University of Technology, Ma'anshan 243002, China

Copyright © 2023 American Foundry Society
<https://doi.org/10.1007/s40962-022-00940-4>

Abstract

Water-soluble cores are an effective solution for complex inner cavity castings due to its excellent ability of leaching out in water. Compared with the rapid development of 3D printing sand mold/core, the water-soluble core additive manufacturing technology is limited by its material properties because water-soluble inorganic salt materials tend to agglomerate and are transparent for the visible and near-infrared lasers. In this study, a process based on direct jetting potassium carbonate solution onto powder bed mix with ceramic sand and bentonite followed with post-treatment was proposed to prepare the water-soluble sand core. The mechanical property of the core was detected in different stages of the forming process, and the mechanism of strength and collapse was analyzed with the aid of phase diagram and scanning electron microscopy. The results show that the strength of binder jetting core exceeds 2 MPa after sintering at 900 °C for 10 min via pre-

sintering and soaking, and the residual strength of the core decreases to 0.12 MPa, which guarantees the leachability of the core out of a casting under a slight vibration. Liquid bridge between sand grains built up in the process of binder jetting transforms into K_2CO_3 bonding bridge during the heating process, and a reticular structure of $KAlSi_mO_n$ grows up with the increase of sintering temperature and the extension of time, which explains the pre-sintered core maintains the original shape in K_2CO_3 solution and the sintered core has a low strength after soaking in water. What is more, a casting trial of tee pipe was conducted to verify the suitability of the developed cores for aluminum alloy castings with complex internal cavities.

Keywords: water-soluble core, binder jetting, potassium carbonate, bonding bridge, strength

Introduction

Water-soluble core is a kind of core for forming the internal surface of castings, which is made from refractory aggregate bonded with water-soluble binder or totally water-soluble material fabricated by casting, press-sintering and binding, in order to satisfy the production of

castings for high temperature and the ability of leaching out in water for core removing. Water-soluble cores had been extensively researched from the 1970s to the 1990s, but few studies were reported in the following decades. Recently, however, water-soluble core has been paid high attention again in the field of gravity casting,^{1,2} low pressure casting and even high pressure die casting,³⁻⁶ because of its characters of excellent collapsibility and convenient recycling.

Yaokawa¹ melted composite salts of 30 mol% NaCl and 70 mol% Na₂CO₃, and then poured into mold to form salt core with 30 MPa. Liu⁷ used MgSO₄ as binder and made water-soluble core with good strength and excellent collapsibility in water. Harper⁸ fabricated the water-soluble core by compression molding with NaCl and water-soluble trehalose binder. The obtained core exhibited a strength of 57 MPa and was successfully used to produce a representative hollow section of an integrally stiffened panel. In the previous study, our team⁹ manufactured a kind of water-soluble core with high strength and low moisture absorption by hot-pressing followed a treatment of precipitation using K₂CO₃ as binder and diatomite/aluminum borate whisker as enhancers, which satisfied the casting of aluminum alloy. In fact, molding molds are essential for both the melt casting and the press sintering processes. Therefore, these methods are not suitable for new product development, due to the high capital costs for tooling and the slow production cycle.

3D printing technology can effectively solve the above problems, so it has attracted much attention in the molding of water-soluble cores. However, the commonly used laser-based 3D printing process does not apply in molding water-soluble cores because water-soluble inorganic salt materials are transparent to visible and near-infrared light.¹⁰ As a result, the micro-drop jetting process is the currently available route for the preparation of water-soluble cores. Moreover, compared to laser-based 3D printing process, binder jetting technology has many advantages in new product development and small-batch production rapid casting process, such as less equipment investment, low operation cost, simple equipment maintenance and good environmental adaptability. A ZCast process^{11,12} proposed by Z Corp can form casting mold & core and non-ferrous casting directly with the mixture powder of casting sand, plastic and other additive. ExOne¹³ 3D printers offer solutions for complex and increasing customer demands with an ester-cured alkaline phenolic resole binder, acid-cured phenolic resole binder and water-based alkali-silicate binder. Although these 3D printing process to produce sand molds/cores already has mature business applications, the water-soluble cores of 3D printing were relatively less reported. Marutani¹⁰ employed 3D printing technology to fabricate water-soluble core with materials such as salt powder, plaster & ceramic slurry and flour. Exone¹⁴ developed X1 Washout which could quickly print sand cores with complex designs, and the cores could be washed out with water after being used. However, these sand cores were used as sacrificial patterns for investment casting or manufacturing carbon fiber, fiberglass or ceramic matrix composites as its maximum cure temperature was lower than 177 °C. Zhao¹⁵ prepared ceramic core by 3D printing the green body of calcium oxide followed with a high temperature sintering using the ethanol solution of phenolic resin with dispersed nano-zirconia particles as binder, but the use of nano-zirconia and phenolic resin definitely

resulted in high cost and the release of carbon emissions. Fan¹⁶ fabricated water-soluble cores with Na₂SO₄-NaCl and bauxite powder by layered extrusion forming, and its excellent comprehensive performance satisfied the requirements for manufacturing hollow composite structure castings. However, the eutectic temperature of Na₂SO₄-NaCl is about 630 °C, which limits its application. In fact, water-soluble cores can be produced by different kinds of water-soluble materials which meet the requirements of different alloy casting. Leonid¹⁷ compared and analyzed the performance of cores made with a modified two-component binder systems with solid silicates instead of traditional liquid silicates by different processes, involving two 3DP process methods by jetting water on the surface of mixing fine sand and solid silicates, and of coating fine sand with solid silicates. However, inorganic salts are susceptible to moisture absorption, and crystal bridges form in the liquid bridges between sand grains when changes in temperature or humidity cause water to evaporate, leading to caking phenomena.¹⁸ Therefore, the two-component process proposed by Leonid is a good process for molding water-soluble cores except for the possible caking in environments with high relative humidity.¹⁷

In order to avoid the caking of sand coating with water-soluble inorganic salt on the powder bed in the two-component binder jetting process, a process based on direct jetting of K₂CO₃ solution onto powder bed mixed with ceramic sand and bentonite was employed to fabricate water-soluble sand cores. Since the powder material and the binder are stored separately and supplied in different paths (spreading by a roller and spraying from a spray-head), there is no caking problem, and the cores satisfy the requirements of gravity casting and low-pressure casting. The effects of process formulation and parameters on tensile strength and water collapsibility were systematically investigated. Moreover, the microstructures of water-soluble core were analyzed by scanning electron microscopy (SEM), and the bonding mechanism was disclosed.

Experimental Procedures

Materials and Equipments

The raw sand was ceramic foundry sand, which was a manufactured Al₂O₃ (≥75%) and SiO₂ (12–25%) main constituents' product with 70/140 meshes and 69 GFN. The binder was consisted of analytical pure potassium carbonate and water. The sodium bentonite was 400 mesh. The forming equipment was the self-developed 3D printer equipped (as shown in Figure 1c) with a resistive heating element fixed on the lift table in working space (as shown in Figure 1b). The spray-head is made by removing the ink from a generic office printer spray-head, cleaning it and filling it with K₂CO₃ solution. The sand mixer was the SHY resin sand mixer (as shown in Figure 1a) from Wuxi

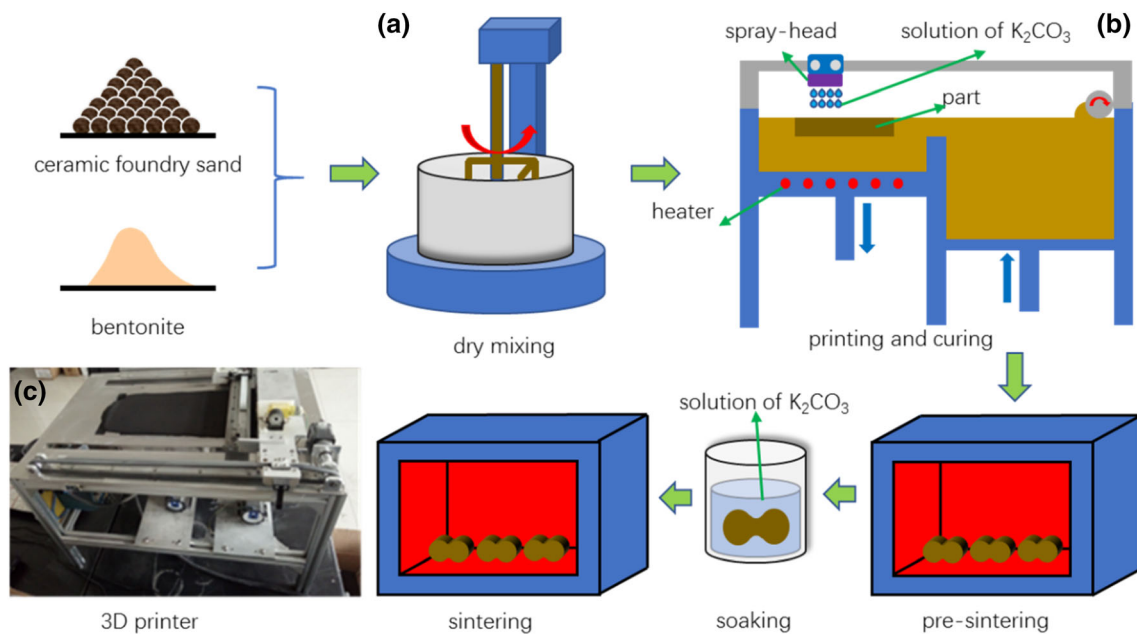


Figure 1. Process of preparing the sand samples.

Sanfeng instrument Equipment Co., Ltd. The sand samples were fabricated as a standard figure “8” dog-bone specimen with the dimension of 22.36×11.18×66.0 mm. Other test equipment included the rotary viscosimeter, the contact Angle measurement instrument, the SWY universal hydraulic strength testing machine, scanning electron microscopy (SEM, FEI Co., Ltd., Netherlands). The dynamic viscosity of the solution was measured by a rotary viscometer. Contact angle was measured by the optical contact angle measuring device of the DataPhysics OCA based on the sessile drop-method.

Preparation of Sand Samples and Properties Test

The process of preparing the sand samples shown in Figure 1. Firstly, ceramic foundry sand and bentonite were dry-mixed in an SHY resin sand mixer for 3 min and then transferred onto the platform of self-developed 3D printer equipped with a resistive heating element. The weight percentage of bentonite was 0, 3 and 5 wt%, respectively. Secondly, the standard figure “8” dog-bone sand specimen samples were printed using a layer thickness of 0.35 mm with the potassium carbonate solution binder concentrations of 30, 40 and 50 wt%, and then the printed sand samples were heated under the temperature of 140, 160 and 180 °C for 1 h. Thirdly, the sand samples were pre-sintered at the temperature of 850 °C for 10 min. Fourthly, the sand samples were soaked in potassium carbonate solution with the concentrations of 30, 40, 50 and 55 wt%, and sintered at the temperature of 750, 800, 850 and 900 °C for 10 to 80 min for the second time. Finally, the samples were soaked in water for 60 min to measure the residual strength which

represented the water-soluble collapsibility. Initial strength, pre-sintering strength, final strength and residual strength is the tensile strength of the samples cooled to the room temperature after heating on the platform, sintering for the first time, sintering for the second time and soaking in water, respectively. In order to verify the molding and collapse performance, the water-soluble core for complex tee pipe casting was printed according to the optimized formulation and process parameters, and a casting test was conducted with scrap aluminum at a pouring temperature of 700 °C.

Results and Discussion

Dynamic Viscosity of K_2CO_3 Solution

Table 1 shows the dynamic viscosity and surface tension and contact angle of K_2CO_3 solution at room temperature. As shown in Table 1, the dynamic viscosity, contact angle and surface tension all increase with the increase of K_2CO_3 solution concentration. According to the Washburn equation which is commonly used to estimate capillary pore infiltration dynamics of powder beds, the penetration/infiltration time t is determined by¹⁹:

$$t = \frac{2L^2\eta}{\gamma r \cos\phi} \quad \text{Eqn. 1}$$

where L is the penetration length/depth, η is the dynamic viscosity, γ is the surface tension, r is the capillary pore radius, and ϕ is the contact angle between the solid capillary and penetrating liquid or dynamic contact angle.²⁰

Equation 1 suggests that the penetration/infiltration time has a proportional relationship with viscosity and an inverse relationship with surface tension. Although the determination of ϕ is difficult, the consensus is that the dynamic contact angle has a relationship of monotone increasing with the liquid viscosity.²¹ As the K_2CO_3

solution has good wettability on the surface of ceramic sand, the value of ϕ is between 0 and 90°. Thus, the static contact angle can replace the dynamic contact angle for a qualitative analysis. Table 1 also lists the value of $\eta/\gamma\cos\theta$, which increases with the increasing of K_2CO_3 solution concentration. It suggests that: the highly concentrated solution takes a much longer time to gain the same penetration depth.

Table 1. Physical Parameters of Solutions with Different Concentrations

K_2CO_3 solution concentration C (%)	Dynamic viscosity η ($\times 10^{-3}$ Pa.s)	Contact angle θ (°)	Surface tension ²² γ ($\times 10^{-3}$ N/m)	$\frac{\eta}{\gamma\cos\theta}$ (s/m)
0	1.033	29.6	72.0	0.014
30	2.673	33.1	83.8	0.032
40	4.058	40.9	91.4	0.045
50	7.336	62.7	103.8	0.075
55	11.483	71.5	–	–

Effect of 3D Printing Process on Tensile Strength

The initial strength of samples with 0, 3 and 5 wt% bentonite at different heating temperatures as a function of K_2CO_3 solution concentration is shown in Figure 2. As shown in Figure 2a, the initial strength of water-soluble cores firstly increases and then decreases with the increase of K_2CO_3 solution concentration and heating temperature. The strength of the sand samples is determined by the bonding quantity and strength of K_2CO_3 generated in the evaporative crystallization. When samples are heated at the

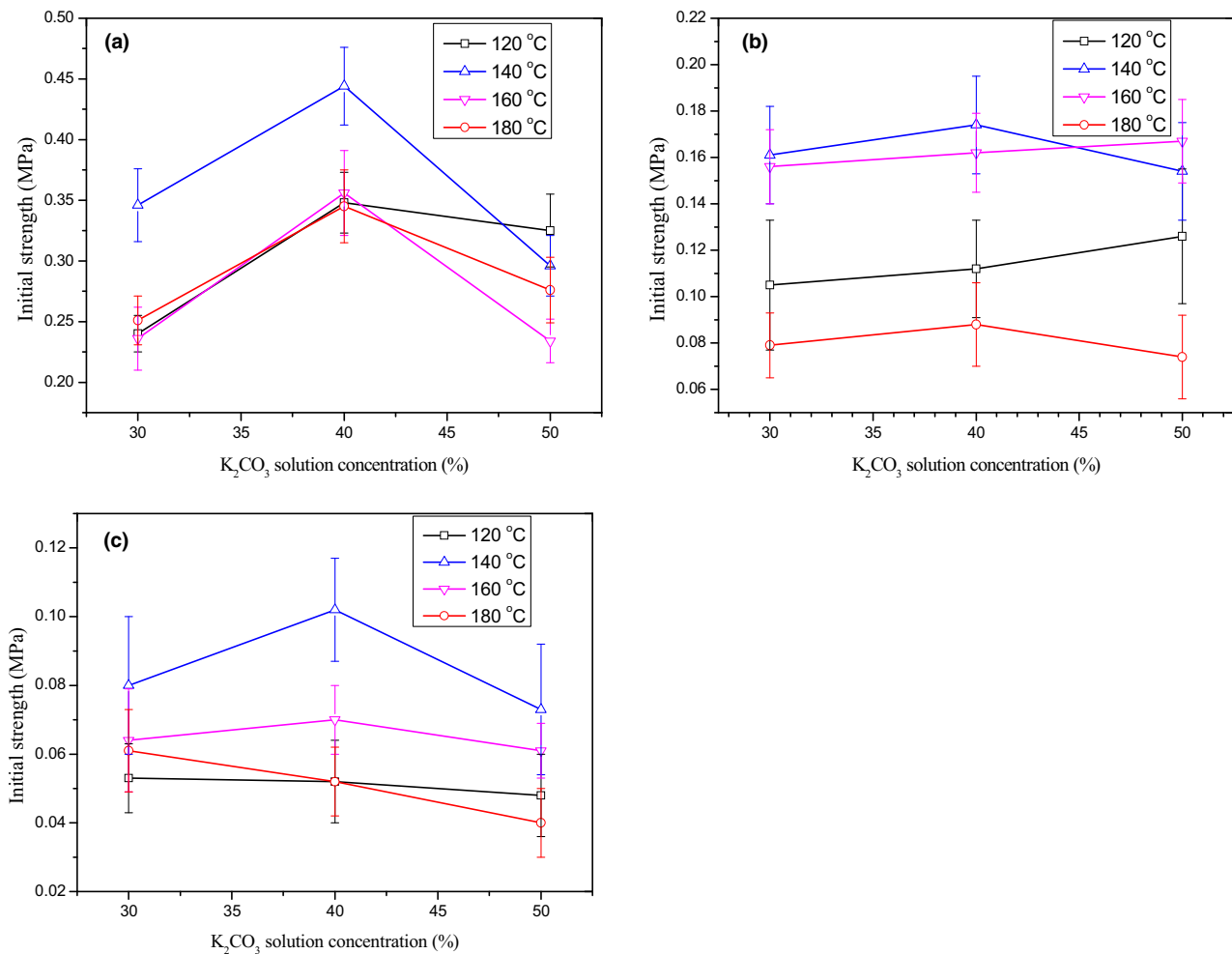


Figure 2. Effect of K_2CO_3 concentration and heating temperature on tensile strength of WSCs with (a) 0 wt%, (b) 3 wt% and (c) 5 wt% bentonite.

same temperature, the crystallization products are identical, which results in the same bonding strength. As the solution concentration increases, the number of bonding bridges increases, resulting in an increase in initial strength. However, the viscosity of K_2CO_3 solution also rises with the increase of solution concentration (as shown in Figure 2), which gives rise to a bad permeability and eventually results in the weak coating effect and low initial strength. Under the action of these two mechanisms, the initial strength reaches maximum at the concentration of 40 wt%. The heating temperature affects the loss of water in solution, so it also has an effect on the initial strength. The low heating temperature slows the evaporation velocity of water in K_2CO_3 solution, which decreases the crystallization velocity; while the high heating temperature accelerates the water evaporation of the samples, which accounts for the cracks on the bonding bridge. As a result, the initial strength reaches maximum at 140 °C at the concentration of 40 wt%. As shown in Figure 2b, c, both the solution concentration and the heating temperature have no significant effect on the initial strength. However, the initial strength of the samples with 3 and 5 wt% bentonite is obviously lower than that with no bentonite under the same situation. The reason is that the quantity of bonding bridge decreases at a given amount of binder injection, as the infiltration capacity of binder solution decreases with increasing bentonite because of its higher specific surface area and adsorption capacity than sand grains. In brief, the initial strength fabricated by 3D printing is low and it is indispensable to conduct a post-treatment process to the samples. In this study, the layer thickness of 0.35 mm, the binder solution concentration of 40 wt%, the heating temperature of 140 °C and the heating time 60 min were selected for the subsequent experiments.

Effect of Bentonite on Pre-Sintering Strength

Samples prepared in “Effect of 3D Printing Process on Tensile Strength” section with different bentonite additions were pre-sintered at 850 °C for 10min. Figure 3 reveals that the bentonite content has a significant effect on the tensile strength before and after pre-sintering. The initial strength is much higher than the pre-sintering strength when no bentonite is added, whereas the initial strength is pretty lower than the pre-sintering strength when the addition content of bentonite is 3 and 5 wt%. It indicates that bentonite has a capability to keep the pre-sintering strength.

Figure 4 shows the phase diagram of K_2CO_3 - H_2O salt-water system according to the solubility data from the reference.²² When the ratio of temperature to water loss is high, anhydrous K_2CO_3 directly crystallizes out of the

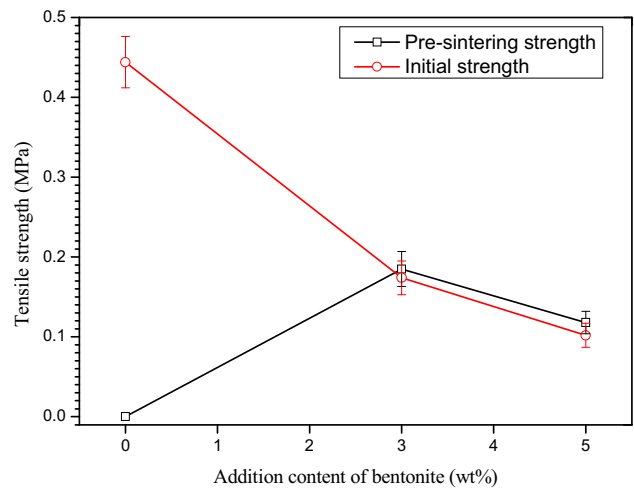


Figure 3. The addition content of bentonite on the tensile strength of the samples before and after pre-sintering process.

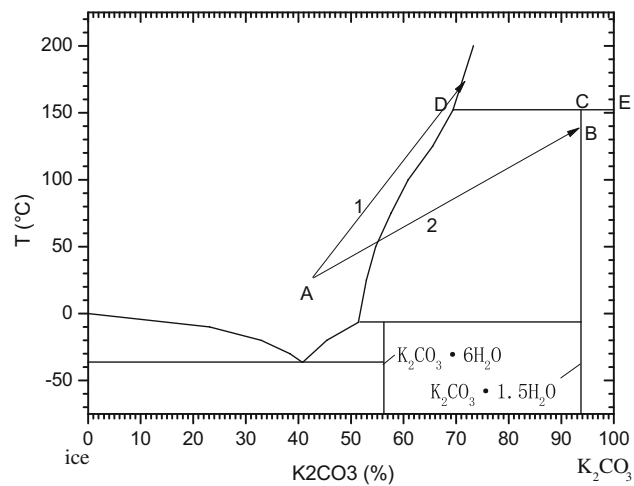


Figure 4. Phase diagram of K_2CO_3 - H_2O salt-water system.

solution along the path 1. On the contrary, when the ratio of temperature to water loss is low, $K_2CO_3 \cdot 1.5H_2O$ firstly crystallizes out of the solution along the path 2, and then turns into anhydrous K_2CO_3 and K_2CO_3 solution at the temperature of 152 °C. It is difficult to measure the ratio of temperature to water loss. However, it must be $K_2CO_3 \cdot 1.5H_2O$ that crystallized out from the solution of K_2CO_3 , as the cores were prepared at 140 °C.

During the pre-sintering process, $K_2CO_3 \cdot 1.5H_2O$ coated on the surface of sand grains transforms into anhydrous K_2CO_3 . When the temperature exceeds 152 °C, K_2CO_3 solution permeates and leads to less bonding bridges among the sand grains. It accounts for the strength decline of cores without bentonite, as shown in Figure 3. However,

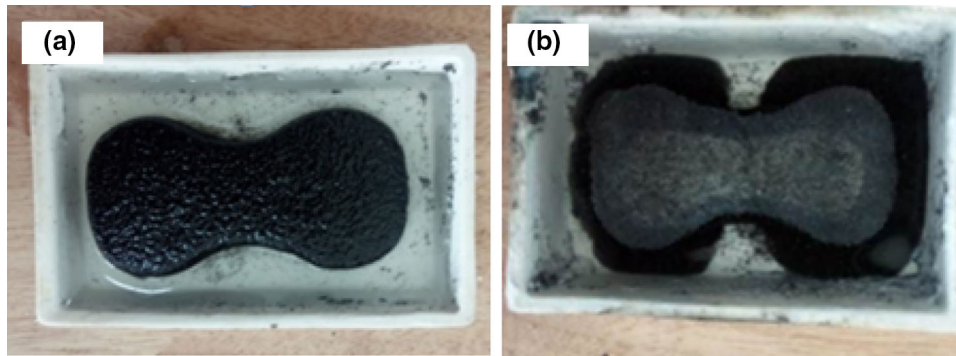


Figure 5. The morphology of the sample soaked in K_2CO_3 solution (a) with pre-sintering; (b) without pre-sintering.

cores with bentonite can hold back the penetration of the K_2CO_3 solution because the bentonite has good absorption capacity, which prevents the solution infiltration so as to maintain the strength of the cores. Although the pre-sintering process has no obvious effect on tensile strength, it guarantees the samples against collapse during soaking in the K_2CO_3 solution for 1 minute, as shown in Figure 5a. According to Figure 5b, the sample without pre-sintering process collapses when it is soaked in the K_2CO_3 solution for 1 min. Therefore, the 3 wt% bentonite was selected to print the cores, and the as-printed cores were pre-sintered at 850 °C for 10 min, and then soaked in K_2CO_3 solution for 1 min.

Effect of K_2CO_3 Solution Concentration on Final Strength

Figure 6 shows the effect of solution concentration on final strength of samples prepared in “Effect of Bentonite on Pre-Sintering Strength” section and sintered at 850 °C for 30 min. As shown in Figure 6, the final strength firstly increases and then decreases with increasing concentration of K_2CO_3 solution, and the tensile strength can reach a maximum of 2.28 MPa with the solution concentration of 50 wt%.

Figure 7 demonstrates the fracture micrograph of the core soaked with different solution concentration. When the K_2CO_3 solution concentration is 30 wt%, all the sand grains present a loose state in Figure 7a, and only a little fracture with small area can be found on the surface of sand grains, which means the bonding bridge is small and weak. When the solution concentration is increased to 40 wt%, as shown in Figure 7b, the quantity of fracture and bonding bridge increases and the sand grains are coated with the inorganic salt, but the arc transition is small. Although holes can still be found, the sand grains present a much

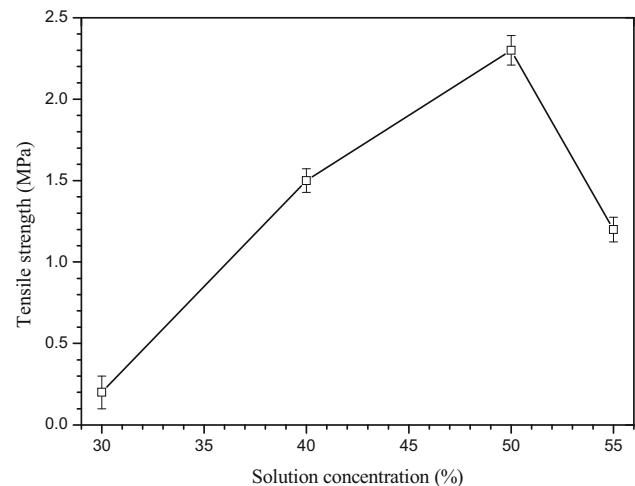


Figure 6. Effect of K_2CO_3 solution concentration on final strength.

denser state. When the solution concentration is 50 wt%, the core exhibits the densest state. Moreover, a large number of fracture and bonding bridges with good arc transition are present in Figure 7c. It can be concluded that crystallization product generated from the solution increases with the increase of the K_2CO_3 solution concentration, which improves the final strength. When compared with Figure 7c, the core in Figure 7d also shows a dense state, but the quantity of fracture is fewer and the bonding bridge does not show the form of good arc transition, which attributes to the lowest fluidity or the highest viscosity of the binder. Thus, the core soaked in a solution concentration of 50 wt% performs the highest strength.

Effect of Sintering Process on Final Strength

The final strength of samples sintered at 750–900 °C for 10–80 min was investigated. As shown in Figure 8, the

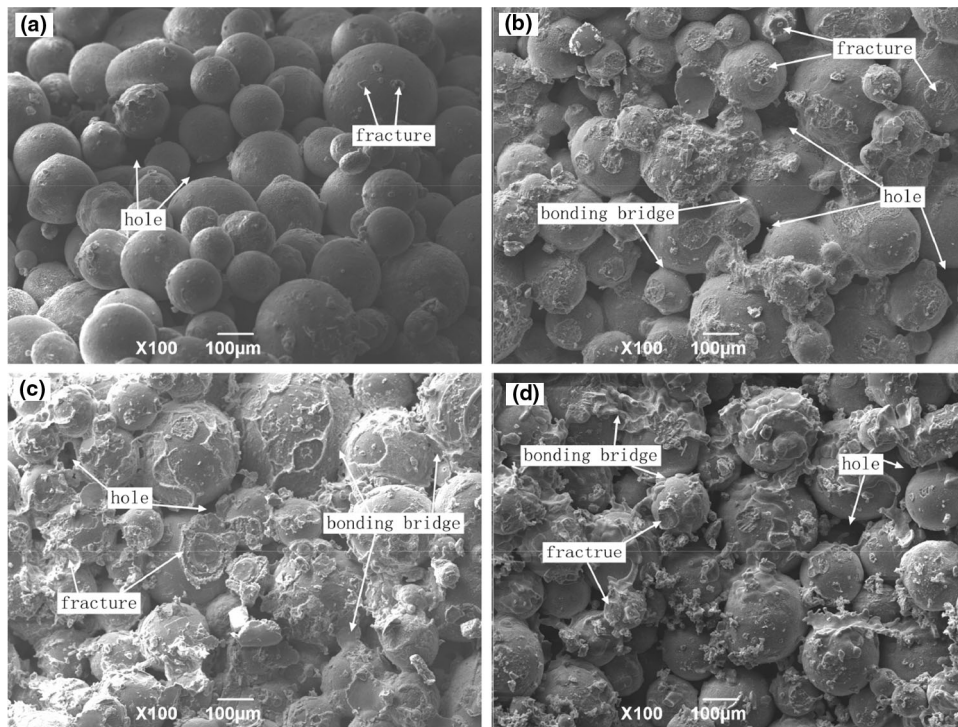


Figure 7. Fracture morphology of the core soaked in different K_2CO_3 solution concentration: (a) 30 wt%, (b) 40 wt%, (c) 50 wt% and (d) 55 wt%.

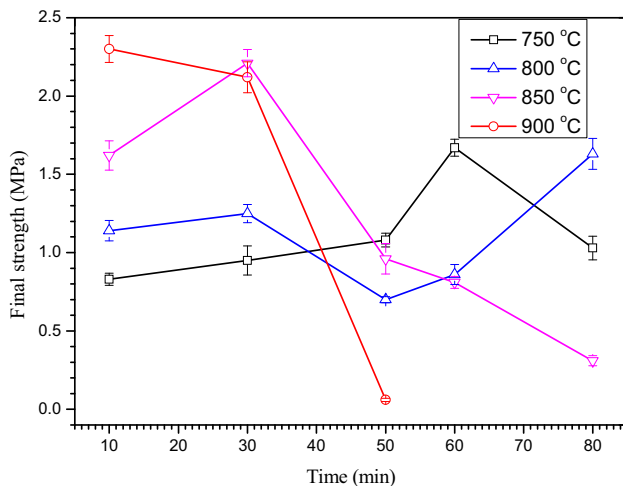


Figure 8. Effect of sintering process on final strength.

final strength of samples is evidently improved compared to the pre-sintering strength. When the sintering temperature is low (750 °C or 800 °C), the final strength is about 0.7-1.7 MPa. When the sintering temperature is high (850 °C or 900 °C), the final strength of the samples is relative high and exceeds 2 MPa. However, the final strength decreases sharply when the samples are sintered at the high temperature for a long time.

Al_2O_3 and SiO_2 are the main compositions of the sand grains and bentonite. Thus, the chemical reaction involved in the core sand mixture with K_2CO_3 are mainly as follows:

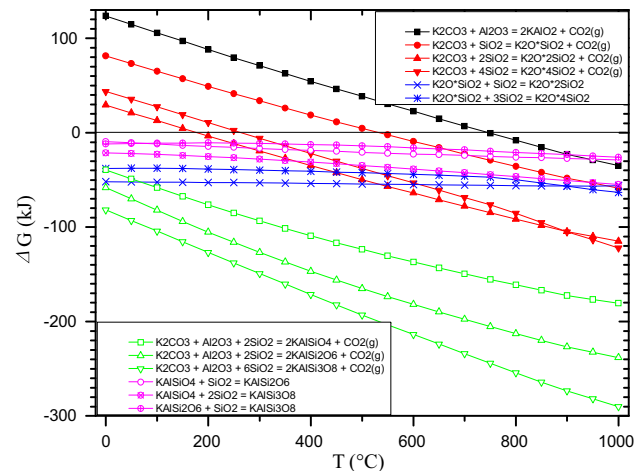
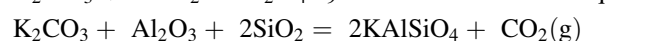
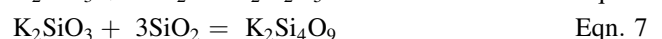
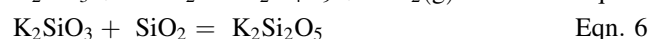
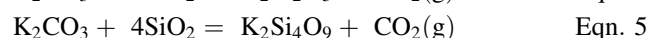
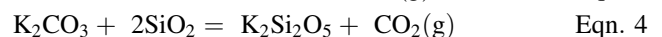
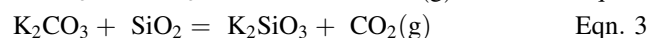
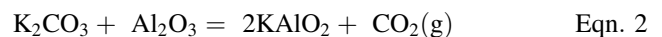


Figure 9. Gibbs free energies variation of reactions.



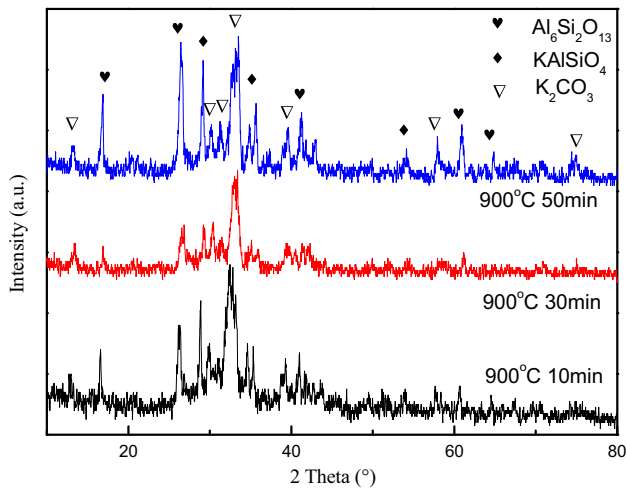


Figure 10. X-ray diffraction pattern of the water-soluble core sintered at 900 °C for 10, 30 and 50 min.

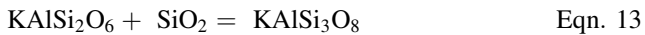
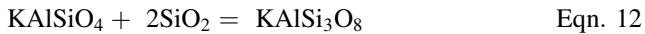
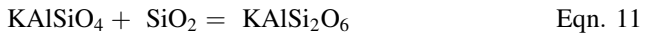
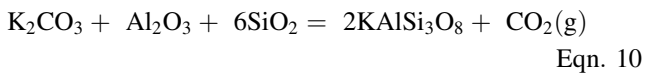
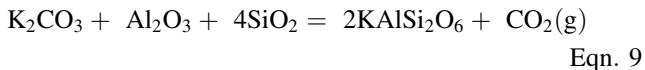


Figure 9 shows the Gibbs free energies variation of reactions between K_2CO_3 and oxides at 0–1000 °C. From the thermodynamic point of view, K_2CO_3 tends to act with oxides (Al_2O_3 and SiO_2) and produces KAISi_mO_n . Figure 10 shows the X-ray diffraction pattern of the water-soluble core sintered at 900 °C for 10, 30 and 50 min. $\text{Al}_6\text{Si}_2\text{O}_{13}$ and K_2CO_3 are the main components of ceramic sand and bonding bridge. The new phase of KAISiO_4 verified the kinetic of reaction between K_2CO_3 and oxides.

Figure 11 displays the fracture morphology of the core sintered at 750–900 °C for 10–80 min. Overall, sand grains are coated well at the fracture section, between which are the bonding bridges with smooth arc transition. Cracks are widespread, but the locations of their appearance are different. When the sintering temperature is low and sintering time is short, cracks mainly appear in the bonding bridges and the necking phenomenon is observed as well, as shown in Figure 11a–e and g. When the sintering temperature is high and the sintering time is long, there are many straight cracks on the surfaces of sand grains, as shown in Figure 11f and h–l. K_2CO_3 content and its sintering reaction with Al_2O_3 and SiO_2 are involved in the improvement of

sintering strength. On one hand, the soaking process increases the K_2CO_3 content, and K_2CO_3 crystallized out of the solution thickens the bonding bridge during the later heating process. On the other hand, K_2CO_3 can react with Al_2O_3 and SiO_2 in the ceramic sand and bentonite to form KAISi_mO_n . Table 2 shows the energy dispersive X-ray (EDX) analysis of water-soluble cores. As can be seen from Table 2, when cores were sintered at different temperatures for different times, the energy spectrum at the fracture is similar, i.e., high content of Al, Si and O elements, and low content of K element, such as point 1,3,5, and 7. However, under low temperature and short time conditions, the energy spectrum of point 2 and 4 on the sand surface expresses a high K and O content and a low Al and Si content, which indicates that the reaction is not sufficient and the bonding film on the sand surface is dominated by K_2CO_3 . In contrast, when the cores were sintered at 850 °C and 900 °C for 30 minutes, the energy spectrum results at points 6 and 8 shows a significant increase in the content of Al and Si element, which indicates a sufficient sintering reaction and the presence of KAISi_mO_n in the bonded film. As the reaction is controlled by diffusion, the reaction product content increases with the rise of temperature and the extension of time and easily reaches the maximum at a high temperature in a short time. When the samples are sintered at the high temperature for a long time, the smooth cracks presented in the coating layer indicate that there is a great thermal stress between the new generated fragile phase and the sand grains, which accounts for the strength decrease.

Residual Strength

Figure 12 illustrates that the residual strength of the samples soaked in water for 60 min increases with increasing sintering temperature. It is clear that, K_2CO_3 solution ejected from spray-head coats ceramic sand grains and bentonite particles, and forms a liquid bridge between sand grains, as shown in Figure 13a. In the subsequent heating process, the water in the solution evaporates and the crystal of K_2CO_3 seed out, so as to form a bond bridge between sand grains to establish its strength, as shown in Figure 13b. During the pre-sintering process, a thin layer of reaction product forms on the sand grains and bentonite particles, and a reticular structure of KAISi_mO_n appears (as shown in Figure 13c), which prevents the dissolution of K_2CO_3 , avoiding the collapse of cores soaking in K_2CO_3 solution. The process of soaking increases the content of K_2CO_3 , which increases the thickness of KAISi_mO_n and decreases the hole diameter of the reticular structure. When the sintering time is the same, the higher the sintering temperature, the faster the reaction rate. Thus, when the

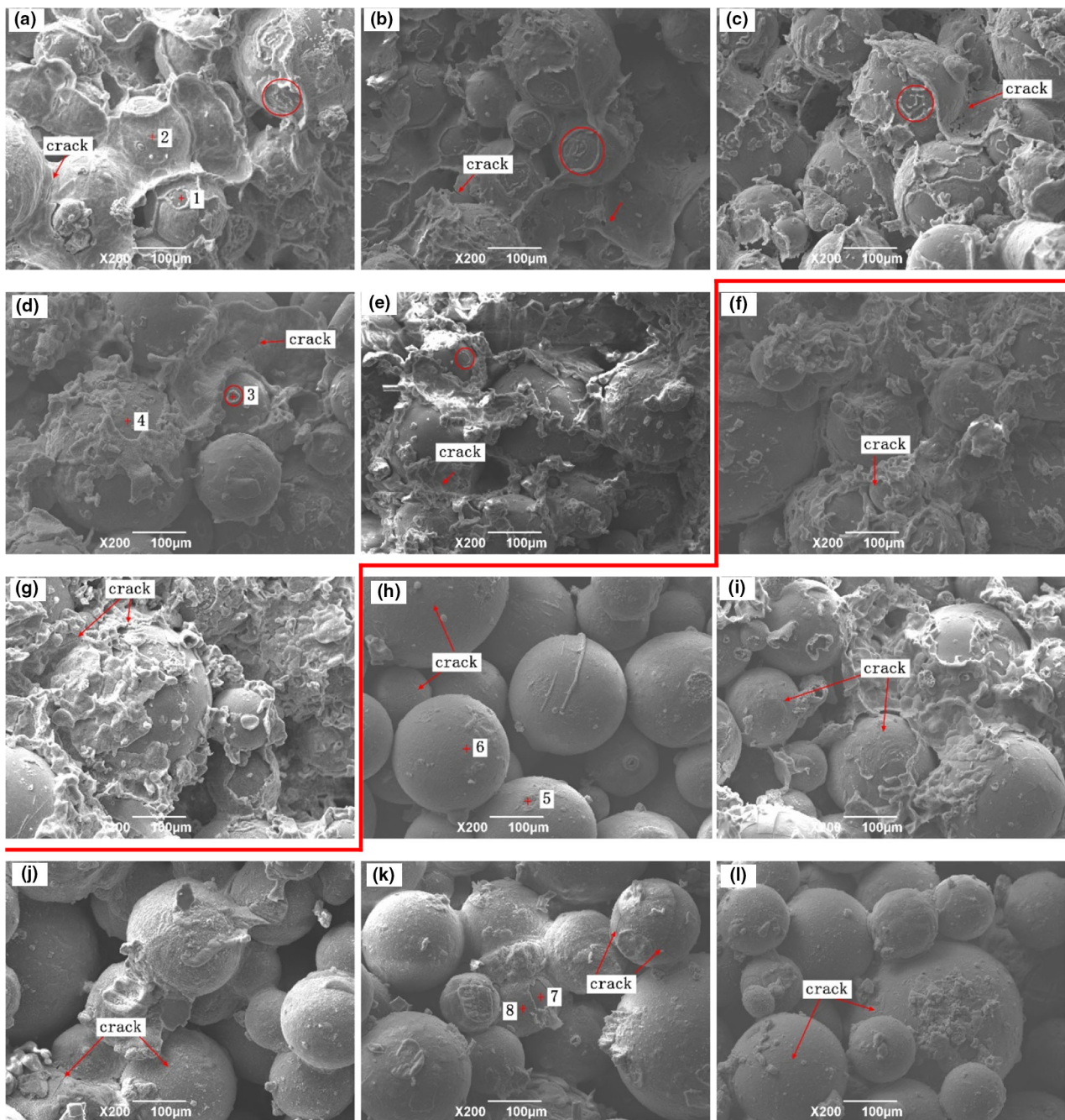


Figure 11. Fracture morphology of the core with the sintering process. (a), (b), (c) sintered at 750 °C for 10, 30 and 80 min; (d), (e), (f) sintered at 800 °C for 10, 30 and 80 min; (g), (h), (i) sintered at 850 °C for 10, 30, 60 min; (j), (k), (l) sintered at 900 °C for 10, 30, 50 min.

samples sintered at 750 °C for 10 min, a three-dimensional reticular structure of KAlSi_mO_n begins to growing up, but most of the K_2CO_3 crystal has not involved in the reaction and still keeps the original structure, which can dissolve easily in the water and leads to a low residual strength. While the samples sintered at 900 °C for 10min, the new produced phase KAlSi_mO_n forms a thick reticular structure

with K_2CO_3 crystal closed in (as shown in Figure 13d) and its strength must be weakened by soaking in water for a long time, which makes the samples show a relatively high strength. However, the strength of the core soaked in water is rather low, which guarantee the leachability of the core out of a casting under a slight vibration.

Table 2. Energy Dispersive X-ray (EDX) Analysis of Each Point in Figure 11

Number	Atom (%)					
	C	O	Al	Si	K	Ti
1	13.18	44.72	29.42	7.81	3.89	0.99
2	23.08	43.59	—	—	33.33	—
3	—	59.19	29.55	9.27	0.73	1.26
4	12.72	57.18	7.33	8.97	13.80	—
5	13.59	45.24	27.70	9.69	1.54	2.24
6	10.31	43.71	8.63	13.12	23.36	0.87
7	21.64	37.14	31.24	5.73	2.48	1.77
8	9.41	37.35	15.06	9.10	29.08	—

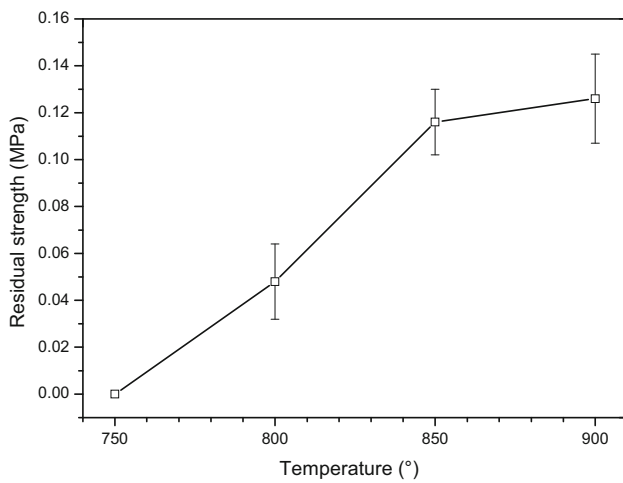


Figure 12. Effect of sintering temperature on residual strength.

Manufacturing of Complex Internal Cavity Castings

Water-soluble cores consisting of ceramic sand mixed with 3% bentonite was printed in 50 layers with a layer thickness of 0.35 mm, using a 40 wt% K_2CO_3 solution as a binder, and then heated at 140 °C for 1 hour. The as-printed cores were applied to casting the complex internal cavity castings via pre-sintering at 850 for 10 min, soaking in 50 wt% K_2CO_3 solution and sintering at 850 for 1 h. Figure 14a shows a water-soluble core coated with mold release agent and fixed in the metal mold of tee pipe. Figure 14b shows the casting in the mold with a large number of air holes on its surface, which must result from the unclean removal of antirust oil from the surface of the mold, and the vaporization after metal casting at a high temperature. When the casting with the core was put into water for 60 minutes, the strength of core decreased rapidly and the core sand could leach out easily with a slight shake. Although the fracture of the core head can also be observed in Figure 14b, it can be seen in Figure 14c that the inner

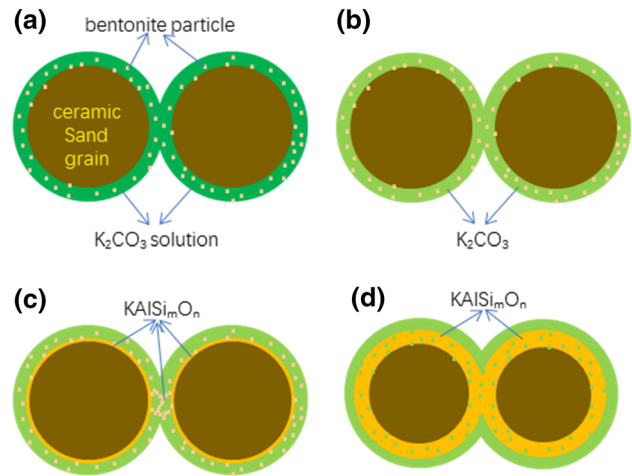


Figure 13. Schematic drawings of the core to build strength. (a) Liquid bridge forms during the binder jetting; (b) bonding bridge forms during the curing; (c) thin reticular structure of $KAlSi_mO_n$ sintered at a low temperature; (d) thick reticular structure of $KAlSi_mO_n$ sintered at a high temperature.

surface of the casting is smooth and clean, with no porosity, metal penetration, chemical scab or other casting defects. Therefore, it can be inferred that the core can withstand the impact of melting metal and is fully suitable for the casting production of aluminum alloy castings with complex internal cavities.

Conclusions

A process based on direct jetting K_2CO_3 solution onto powder bed mixed with ceramic sand and bentonite followed with post-treatment was proposed to prepare the water-soluble sand core. The experimental results could be summarized as follows.

- (1) The strength of binder jetting core exceeds 2 MPa with a residual strength about 0.12 MPa which can apply in aluminum alloy casting followed with the characteristic of easily leaching out. The processing conditions were: 3 wt% bentonite, binder of 40 wt% K_2CO_3 solution, layer thickness 0.35mm, curing at 140 °C for 1 h, pre-sintering at 850 °C for 10 min, soaking in 50 wt% K_2CO_3 solution, sintering at 900 °C for 10 min.
- (2) Liquid bridge between sand grains built up in the process of binder jetting transforms into K_2CO_3 bonding bridge during the heating process, and a reticular structure of $KAlSi_mO_n$ grows up with the increase of sintering temperature and the extension of time, which explains the pre-sintered core maintains the original shape in K_2CO_3 solution and the sintered core has a low strength after soaking in water.

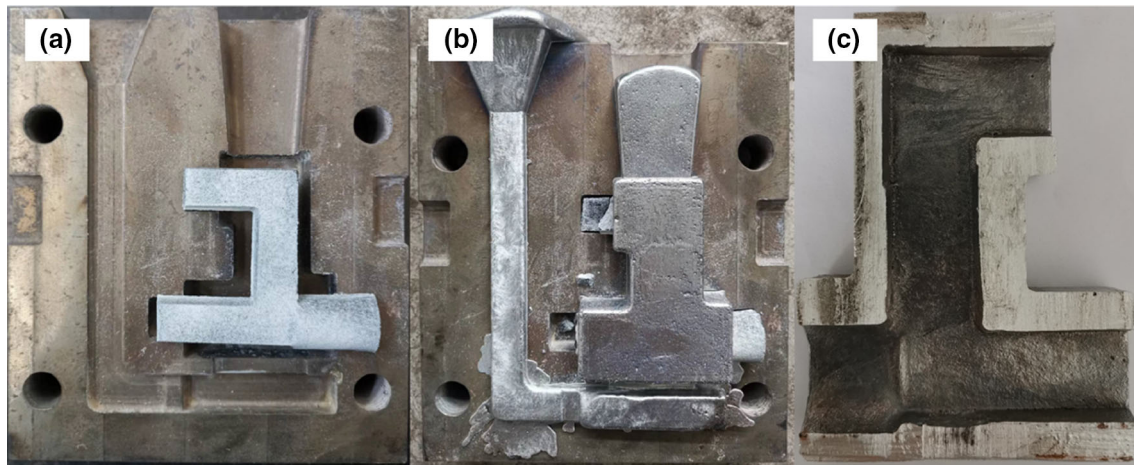


Figure 14. The photo of aluminum alloy casting fabricated by water-soluble core and leached by water. (a) Casting molds with water soluble cores fixed; (b) Aluminum alloy casting with the water-soluble core; (c) Dissected casting.

- (3) The thick reticular structure of KAlSi_mO_n generated under the conditions of relatively high temperature or long time tends to crack on the surfaces of sand grains, which accounts for the decrease of strength with increasing sintering temperature and holding time.

Acknowledgements

This work was jointly supported by grants from the National Nature Science Foundation of China (No. 51405002), Anhui Provincial Natural Science Foundation (No. 2108085ME173) and open funds from Anhui Province Key Laboratory of Metallurgical Engineering & Resources Recycling (No. SKF20-05).

REFERENCES

1. J. Yaokawa, D. Miura, K. Anzai et al., Strength of salt core composed of alkali carbonate and alkali chloride mixtures made by casting technique. *Mater. Trans.* **48**(5), 1034–1041 (2007). <https://doi.org/10.2320/matertrans.48.1034>
2. P. Jiang, F. Liu, Z. Fan et al., Performance of water-soluble composite sulfate sand core for magnesium alloy castings. *Arch. Civ. Mech. Eng.* **16**(3), 494–502 (2016). <https://doi.org/10.1016/j.acme.2016.03.006>
3. R. Huang, B. Zhang, Study on the composition and properties of salt cores for zinc alloy die casting. *Int. J. Metalcast.* **11**(3), 440–447 (2017). <https://doi.org/10.1007/s40962-016-0086-7>
4. B. Fuchs, H. Eibisch, C. Korner, Core viability simulation for salt core technology in high-pressure die casting. *Int. J. Metalcast.* **7**, 39–45 (2013). <https://doi.org/10.1007/BF03355557>
5. F. Liu, S. Tu, X. Gong et al., Comparative study on performance and microstructure of composite water-soluble salt core material for manufacturing hollow zinc alloy castings. *Mater. Chem. Phys.* **252**, 1–10 (2020). <https://doi.org/10.1016/j.matchemphys.2020.123257>
6. S. Tu, F. Liu, G. Li et al., Fabrication and characterization of high-strength water-soluble composite salt core for zinc alloy die castings. *Int. J. Adv. Manuf. Technol.* **95**, 505–512 (2018). <https://doi.org/10.1007/s00170-017-1208-y>
7. F. Liu, P. Jiang, Y. Huang et al., A water-soluble magnesium sulfate bonded sand core material for manufacturing hollow composite castings. *Compos. Struct.* **201**, 553–560 (2018). <https://doi.org/10.1016/j.compstruct.2018.06.084>
8. Z. Xiao, L.T. Harper, A.R. Kennedy et al., A water-soluble core material for manufacturing hollow composite sections. *Compos. Struct.* **182**, 380–390 (2017). <https://doi.org/10.1016/j.compstruct.2017.09.058>
9. L. Zhang, Y. Li, Q. Chen, Optimization of the mixture design of the formula for water-soluble cores. *J. Huazhong U. Sci. Technol.* **39**, 6–9 (2011). (in chinese)
10. Y. Marutani, T. Kamitani, Manufacturing sacrificial patterns for casting by salt powder lamination. *Rapid Prototyp. J.* **10**, 281–287 (2004). <https://doi.org/10.1108/13552540410562313>
11. H. Zhao, Z. Fan, C. Ye, Review of research status for three-dimensional printing technology in review of research status for three-dimensional printing technology in rapid prototyping of powder material. *Aeronaut. Manuf. Technol.* **9**, 42–45 (2011). <https://doi.org/10.16080/j.issn1671-833x.2011.09.008>. (in chinese)
12. A. Koltygin, V. Bazhenov, Development of a substitute for Z cast molding sand used on installations of 3D printing for obtaining aluminum, magnesium, and iron casting. *Russ. J. Non-ferrous Metals* **53**, 38–41 (2012). <https://doi.org/10.3103/S1067821212010129>

13. ExOne, Sand Casting 3D Printing Materials & Binders. <https://www.exone.com/en-US/3d-printing-materials-and-binders/sand>. Accessed 15 July 2022
14. ExOne, 3D Printed Sacrificial Tooling that Washes Out with Water. <https://www.exone.com/en-US/X1-Tooling/X1-Washout>. Accessed 15 July 2022
15. H. Zhao, C. Ye, Z. Fan et al., 3D printing of CaO-based ceramic core using nanozirconia suspension as a binder. *J. Eur. Ceram. Soc.* **37**, 5119–5125 (2017). <https://doi.org/10.1016/j.jeurceramsoc.2017.06.050>
16. X. Gong, X. Liu, Z. Chen et al., 3D printing of high-strength water-soluble salt cores via layered extrusion. *Int. J. Adv. Manuf. Technol.* **118**, 2993–3003 (2022). <https://doi.org/10.1007/s00170-021-08131-x>
17. L. Zaretskiy, Hydrous solid silicates in new foundry binders. *Int. J. Metalcast.* **12**, 275–291 (2018). <https://doi.org/10.1007/s40962-017-0155-6>
18. G. Walker, T. Magee, C. Holland et al., Caking processes in granular NPK fertilizer. *Ind. Eng. Chem. Res.* **37**(2), 435 (1998). <https://doi.org/10.1021/ie970387n>
19. D. Oropeza, R. Roberts, A.J. Hart, A rapid development workflow for binder inks for additive manufacturing with application to polymer and reactive binder ink formulation. *J. Manuf. Process* **73**, 471–482 (2022). <https://doi.org/10.1016/j.jmapro.2021.10.068>
20. Y. Bai, C. Wall, H. Pham et al., Characterizing binder-powder interaction in binder jetting additive manufacturing via sessile drop goniometry. *ASME. J. Manuf. Sci. Eng.* **141**, 1–11 (2019). <https://doi.org/10.1115/1.4041624>
21. X. Wang, X. Peng, B. Wang, A review on dynamic wetting and dynamic contact angle. *J. Basic Sci. Eng.* **11**, 396–404 (2003). <https://doi.org/10.3969/j.issn.1005-0930.2003.04.009>
22. APC The, Potassium Carbonate Handbook. <https://www.armandproducts.com/resources>

Publisher's Note Springer Nature remains neutral with regard to jurisdictional claims in published maps and institutional affiliations.

Springer Nature or its licensor (e.g. a society or other partner) holds exclusive rights to this article under a publishing agreement with the author(s) or other rightsholder(s); author self-archiving of the accepted manuscript version of this article is solely governed by the terms of such publishing agreement and applicable law.